LETTERS

Cryptic chlorination by a non-haem iron enzyme during cyclopropyl amino acid biosynthesis

Frédéric H. Vaillancourt[1]*, Ellen Yeh[1]*, David A. Vosburg[1]†, Sarah E. O'Connor[1]† & Christopher T. Walsh[1]

Enzymatic incorporation of chlorine, bromine or iodine atoms occurs during the biosynthesis of more than 4,000 natural products[1]. Halogenation can have significant consequences for the bioactivity of these products so there is great interest in understanding the biological catalysts that perform these reactions. Enzymes that halogenate unactivated aliphatic groups have not previously been characterized. Here we report the activity of five proteins—CmaA, CmaB, CmaC, CmaD and CmaE—in the construction of coronamic acid (CMA; 1-amino-1-carboxy-2-ethylcyclopropane), a constituent of the phytotoxin coronatine synthesized by the phytopathogenic bacterium *Pseudomonas syringae*[2]. CMA derives from L-*allo*-isoleucine, which is covalently attached to CmaD through the actions of CmaA, a non-ribosomal peptide synthetase module, and CmaE, an unusual acyltransferase. We show that CmaB, a member of the non-haem Fe^{2+}, α-ketoglutarate-dependent enzyme superfamily, is the first of its class to show halogenase activity, chlorinating the γ-position of L-*allo*-isoleucine. Another previously undescribed enzyme, CmaC, catalyses the formation of the cyclopropyl ring from the γ-Cl-L-*allo*-isoleucine product of the CmaB reaction. Together, CmaB and CmaC execute γ-halogenation followed by intramolecular γ-elimination, in which biological chlorination is a cryptic strategy for cyclopropyl ring formation.

Coronatine is a hybrid non-ribosomal peptide-polyketide leaf toxin containing CMA, a cyclopropyl amino acid, itself derived from the non-proteinogenic *allo* diastereomer of L-isoleucine[3,4] (Fig. 1a). A variant of coronatine containing norcoronamic acid (norCMA) derived from L-valine is also produced in low quantities[5]. Although the source of L-*allo*-Ile in *P. syringae* is not known, a cluster of *cma* genes[2,6] is responsible for generating CMA from L-*allo*-Ile by using non-ribosomal peptide synthetase (NRPS) modules (Fig. 1b). Multimodular NRPS enzymes sequester amino-acid monomers through thioester linkage to the phosphopantetheinyl prosthetic group of carrier-protein domains. Downstream domains or dedicated tailoring enzymes may then catalyse modifications of the tethered monomer or peptide bond formation between monomers. Previously, CmaA, which contains NRPS adenylation (A) and thiolation (T) domains, was shown to activate L-*allo*-Ile as the AMP ester and install it on the 10-kDa T domain[6]. We now assign functions to CmaB, CmaC, CmaD and CmaE and reveal the underlying enzymatic logic by which unactivated carbon centres are functionalized by halogenation to facilitate cyclopropyl formation.

CmaD is a stand-alone 8-kDa T domain that lacks a corresponding A domain but may be aminoacylated *in trans* by the A domain of CmaA (see Supplementary Table S2 for kinetic data of the CmaA A domain). After heterologous expression, apo-CmaD is modified post-translationally with the phosphopantetheine arm to generate the holo form of the carrier domain. However, CmaA was unable to transfer L-*allo*-[^{3}H]Ile or L-[^{14}C]Val in the presence of ATP to CmaD, because no radioactivity was associated with the acid-precipitated protein. However, after the addition of CmaE, a 32-kDa protein with homology to the α/β hydrolase superfamily, covalent attachment of these amino acids to CmaD was detected. Autoradiography of the labelled proteins shows time-dependent labelling of CmaA followed by transfer of L-[^{14}C]Val to CmaD by the action of CmaE (Fig. 2a; see Supplementary Methods for detailed assay protocol). A functional CmaA T domain is required because no labelling of CmaD was observed when the S542A variant of CmaA was used for transfer (Ser 542 is the site of modification for the phosphopantetheine attachment; Fig. 2b). CmaE is a previously undescribed acyltransferase that shuttles amino acid groups between T domains. Because

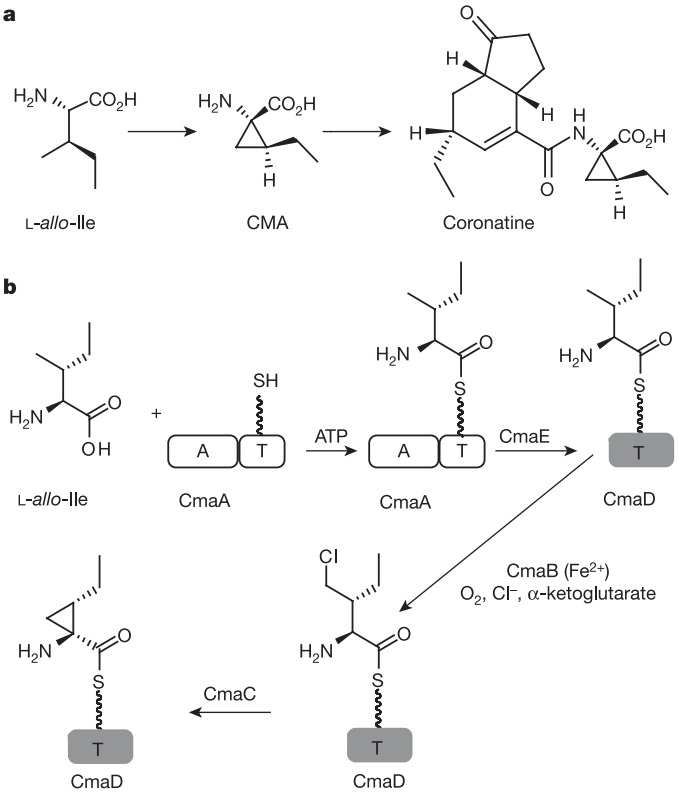

Figure 1 | Biosynthesis of CMA and coronatine. a, The biosynthesis of coronatine from L-*allo*-Ile. **b**, The generation of CMA-*S*-CmaD from L-*allo*-Ile by CmaA, CmaB, CmaC, CmaD and CmaE.

[1]Department of Biological Chemistry and Molecular Pharmacology, Harvard Medical School, Boston, Massachusetts 02115, USA. †Present address: Department of Chemistry, Massachusetts Institute of Technology, Cambridge, Massachusetts 02139, USA (S.E.O.); Department of Chemistry, Harvey Mudd College, Claremont, California 91711, USA (D.A.V.).
*These authors contributed equally to this work.

CmaE itself becomes labelled during the reaction, formation of an acyl-enzyme intermediate through the active-site cysteine (Cys 105) is probably involved. Consistent with this was our observation that loading of CmaD *in trans* is abolished when the variant C105A of CmaE is tested for transfer (Fig. 2b). As discussed below, CmaD, but not the T domain of CmaA, is able to present aminoacyl groups for subsequent transformation by CmaB and CmaC.

A second previously undescribed enzyme in this pathway is CmaB, which has homology to α-ketoglutarate (α-KG)-dependent non-haem Fe^{2+} enzymes that use one Asp/Glu and two His side chains as ligands to oxygen-labile Fe^{2+} (refs 7, 8). These enzymes typically perform oxygenation reactions, but CmaB has the highest degree of homology with other genes potentially involved in the halogenation of syringomycin E and barbamide[9,10]. N-His-tagged CmaB was overproduced in *Escherichia coli* and purified under anaerobic conditions as the apo protein. After cleavage of the His tag with protease, the enzyme was reconstituted with Fe^{2+} and α-KG. The Fe^{2+} content of the holo protein was 81%. After *in trans* loading of CmaD with L-*allo*-[^{3}H]Ile or L-[^{14}C]Val, the aminoacyl-*S*-CmaD was incubated with reconstituted CmaB in the presence of α-KG, Cl^- and O_2. The product was released by thioesterase cleavage[11], derivatized to the *o*-phthalaldehyde/3-mercaptopropionate adduct, and analysed by radio-HPLC. Instead of the cyclopropane-containing CMA (from L-*allo*-Ile) or norCMA (from L-Val), γ-Cl-L-*allo*-Ile or γ-Cl-L-Val, respectively, was formed as judged by co-elution with authentic standards (Fig. 3a–c; see Supplementary Methods and Supplementary Fig. S1 for protocols and synthesis of standards) and liquid chromatography (LC)–MS mass determination of the *o*-phthalaldehyde/3-mercaptopropionate-derivatized amino acid (Fig. 3e). When L-*allo*-[^{3}H]Ile or L-[^{14}C]Val was presented on the carrier-protein domain of CmaA, no chlorinated product could be detected. CmaB specifically recognizes aminoacyl thioester substrates presented on the carrier protein CmaD. Chlorinated product formation by CmaB was dependent on Fe^{2+}, α-KG, O_2 and Cl^- (Fig. 3c). When Cl^- was provided as $Na^{36}Cl$, both the released γ-Cl-L-*allo*-Ile product (Fig. 3c) and γ-Cl-L-*allo*-Ile-*S*-CmaD protein (Fig. 3d) became labelled. CmaB is therefore a non-haem Fe^{2+}, α-KG-dependent halogenase.

Non-haem Fe^{2+}, α-KG-dependent oxygenases have been well characterized[12,13]. CmaB also requires O_2 and α-KG for its reaction but performs chlorination rather than oxygenation at unactivated γ positions of the aminoacyl substrate. A radical pathway is likely, involving the prototypic high-valent oxoiron[14,15] (Fe^{IV}=O) generated in the CmaB active site from O_2-dependent decarboxylation of α-KG. Abstraction of a hydrogen atom, H$^{\cdot}$, from the substrate's γ-position would yield the methylene radical of the substrate and a Fe^{3+} species that could transfer $Cl^{\cdot}$ or $OH^{\cdot}$ to yield a halogenase (Fig. 4a) or oxygenase outcome. Transfer of a hydroxyl or chlorine radical could depend on the orientation of the proposed substrate's $CH_2^{\cdot}$ (γ-position) in the transition state and the placement of the OH and Cl substituents on or near the Fe. A reaction of chromyl chloride with cyclohexane gives an equal yield of $Cl^{\cdot}$ and $OH^{\cdot}$ transfer[16,17], whereas a model iron compound that probably forms an oxoiron species reacts with cyclohexane to yield the chlorinated product specifically[18]. The detection of substrate and chlorine radicals and identification of the iron-based chlorinating agent will be some of the future challenges for this halogenase class. In the CmaB reaction, no hydroxylation product was detected. It was not possible to determine whether substrate hydroxylation would occur in the absence of available chloride ions, because a small amount of chlorinated product is obtained even when the reaction is

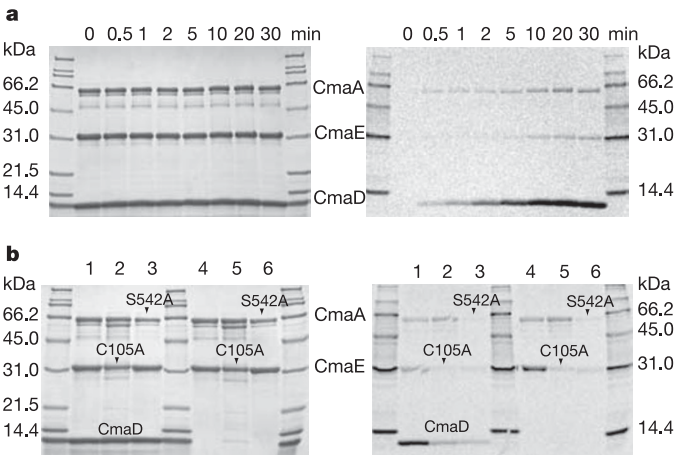

Figure 2 | The transfer of L-Val from CmaA to CmaD catalysed by CmaE. **a**, Time course of the reaction catalysed by CmaE with L-[^{14}C]Val in the presence of CmaA and CmaD. Left, SDS–PAGE; right, autoradiogram. **b**, CmaE was incubated with L-[^{14}C]Val in the presence of CmaA with or without CmaD (lanes 1 and 4). CmaE C105A was incubated with L-[^{14}C]Val in presence of CmaA with or without CmaD (lanes 2 and 5). CmaE was incubated with L-[^{14}C]Val in presence of CmaA S542A with or without CmaD (lanes 3 and 6). Left, SDS–PAGE; right, autoradiogram. All reactions were quenched after a 10-min incubation.

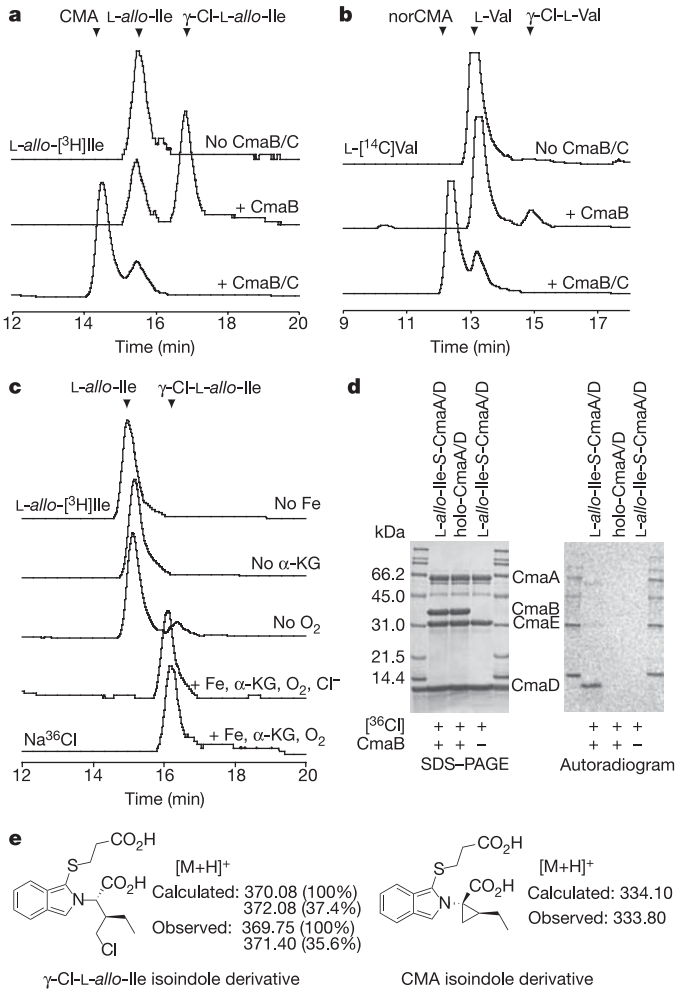

Figure 3 | Analysis of the reactions catalysed by CmaB and CmaC. **a**, HPLC traces of hydrolysed/derivatized amino acid obtained after incubation of L-*allo*-Ile-*S*-CmaD with CmaB and with CmaB plus CmaC. **b**, HPLC traces of hydrolysed/derivatized amino acid obtained after incubation of L-Val-*S*-CmaD with CmaB and with CmaB plus CmaC. **c**, Iron, α-KG, O_2 and Cl^- are required for the CmaB reaction. **d**, Incorporation of $^{36}Cl^-$ into γ-Cl-L-*allo*-Ile-*S*-CmaD by CmaB. **e**, Mass spectrometric analysis of the isoindole derivatives of γ-Cl-L-*allo*-Ile and CMA hydrolysed from CmaD after reaction with CmaB and CmaC, respectively.

performed under chloride-free conditions. Cl^- seems to be retained during protein purification such that its total exclusion is not possible. The γ-chlorination of L-*allo*-Ile and L-Val requires that the amino acids be presented as thioesters tethered to the carrier protein CmaD because free L-*allo*-Ile and L-Val were not chlorinated. A detailed kinetic analysis is complicated by the protein-bound linkages of substrate and product. However, by monitoring the consumption of α-[1-^{14}C]KG, CmaB was active for 16 ± 6 turnovers on L-*allo*-Ile-*S*-CmaD as its substrate. How CmaB recognizes the T domain of CmaD but not the T domain of CmaA remains unclear.

Because formation of the α,γ-cyclopropane ring in CMA and norCMA was shown to proceed through a γ-chloroaminoacyl-*S*-CmaD intermediate, we continued our search for a catalyst that would complete the conversion of the γ-chloroaminoacyl intermediate to CMA or norCMA. CmaC shows sequence homology to methylmalonyl-CoA epimerases[19], a member of the vicinal oxygen chelate superfamily[20,21], which uses the 2-His-1-carboxylate facial triad[7,8] for binding of an active-site Co^{2+} to generate a thioester enolate. When CmaC was overproduced and purified from *E. coli*, it contained a mixture of bound-metal cations in the following ratio: 0.30 equiv. Fe, 0.24 equiv. Zn, 0.11 equiv. Mn, 0.06 equiv. Ni, 0.01 equiv. Cu and 0 equiv. Co. On addition of CmaC to the CmaB-generated γ-chloroaminoacyl-*S*-CmaD product, CMA and norCMA were formed from L-*allo*-[^{3}H]Ile and L-[^{14}C]Val, respectively (Fig. 3a, b). CmaC alone was sufficient to perform this reaction because active CmaB was not required for the final transformation. Although mechanistic analysis remains to be conducted on CmaC, including the role of divalent metal cations, it is very likely that the cyclopropane ring is formed by intramolecular attack of an enzyme-stabilized Cα carbanion on Cγ to displace the chloride ion (Fig. 4b).

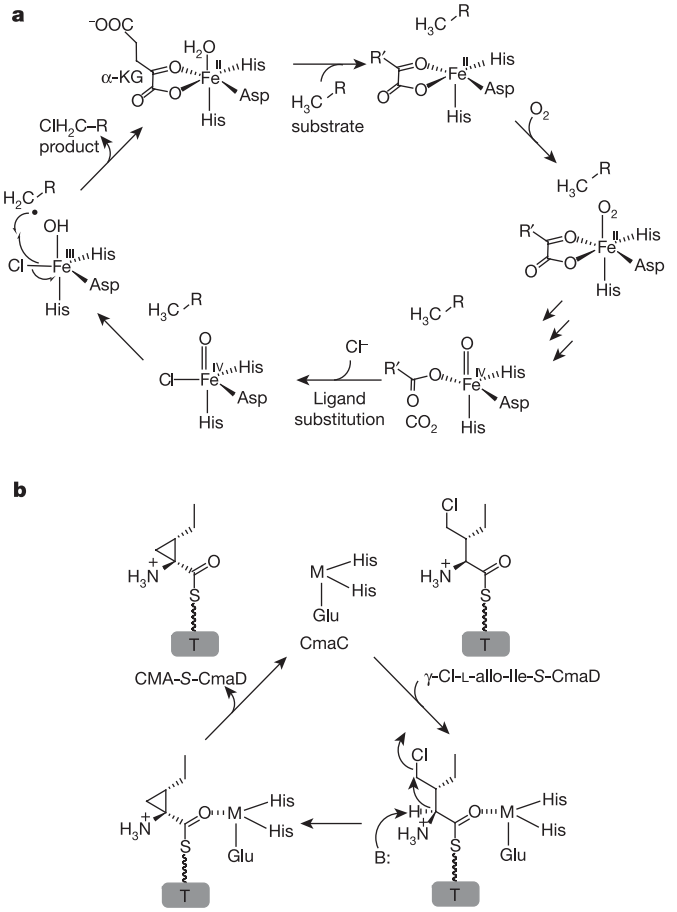

Figure 4 | Proposed mechanisms of CmaB and CmaC. a, Proposed mechanism of halogenation catalysed by CmaB. **b**, Proposed mechanism of cyclopropane formation catalysed by CmaC.

The molecular logic of the CmaA/CmaB/CmaC/CmaD/CmaE pathway, including three previously unknown reactions, is now revealed (Fig. 1b). The A domain of CmaA activates L-*allo*-Ile or L-Val as an aminoacyl-AMP and then installs it by means of a thioester linkage onto the CmaA T domain. CmaE transfers the aminoacyl group from the T domain of CmaA to a second T domain, CmaD, a protein scaffold that is recognized by CmaB. Thus, the aminoacyl substrate is effectively sequestered on a dedicated carrier protein for subsequent enzymatic transformations. The chemical problem of activating the γ-position of aliphatic amino acids is solved by CmaB, a unique non-haem Fe^{2+} halogenase. By a presumptive radical mechanism, enabled by the prototypic Fe^{4+} oxo intermediate of this enzyme class, CmaB regiospecifically chlorinates the substrate at Cγ. The γ-Cl-aminoacyl product remains tethered to CmaD for the final enzyme, CmaC, to generate the kinetically stabilized Cα carbanion adjacent to the thioester. Intramolecular displacement of the γ-Cl group yields the cyclopropyl ring.

The chlorination of L-*allo*-Ile tethered to CmaD is cryptic in the overall pathway of cyclopropyl ring formation. Other biosynthetic clusters that form amino-carboxy-cyclopropane moieties should be inspected for a similar enzymatic strategy. Indeed, we have found such an enzyme sequence in the biogenesis of the apoptosis-inducing cytotrienin A (M. Ueki, F.H.V., S. Garneau, E.Y., D.A.V., H. Osada and C.T.W., unpublished work). Similarly, other members of the non-haem Fe^{2+}, α-KG-dependent enzyme superfamily may be explored for halogenase activity. We have detected halogenase activity in enzyme family member SyrB2 generating the 4-Cl-L-Thr-*S*-enzyme in the biosynthetic pathway of syringomycin[22].

Nature uses both $FADH_2$-dependent and non-haem Fe^{2+} enzymes for hydroxylation, each titrated to the reactivity of the specific substrates[23–25]. It seems that a similar two-pronged strategy is employed for the halogenation of amino acids. For electron-rich aromatic substrates, $FADH_2$-dependent monooxygenases generate FAD-OOH, which is sufficiently reactive for electrophilic oxygen transfer[26]. $FADH_2$-dependent halogenases may form FAD-O-Cl as the proximal chlorinating agent for aromatic substrates[27]. For unactivated aliphatic carbon centres, a more potent oxygen gun in the form of high-valent oxo-iron intermediates is required and generated by Fe^{2+} oxygenases[14]. For the non-haem Fe^{2+} halogenase described here, we presume that the more potent $Fe^{4+}{=}O$ oxygen gun also becomes a more potent halogen gun. O_2 undergoes reductive fragmentation in all these reactions. For substrate chlorination, O_2 fragmentation is used to generate an oxidized form of chloride ion as the reactive chlorinating agent in the active site. The CMA pathway demonstrates Nature's elegant chemical logic for converting an unactivated methyl group to the methylene moiety of a cyclopropane by a cryptic chlorination strategy using five dedicated proteins.

METHODS

Chemicals. L-[^{14}C]Val (250 mCi mmol^{-1}) and Na^{36}Cl (16 mCi g^{-1} Cl) were from American Radiolabelled Chemicals, Inc. L-[^{3}H]*allo*-Ile (1 Ci mmol^{-1}) was from Moravek Biochemicals, Inc. α-[1-^{14}C]ketoglutaric acid, sodium salt (54.5 mCi mmol^{-1}) and [^{32}P]pyrophosphate were from Perkin Elmer Life Sciences, Inc. Coronamic acid was a gift from Ronald J. Parry. γ-Cl-L-valine, γ-Cl-L-*allo*-isoleucine and norCMA were synthesized as described in Supplementary Methods. All other chemicals were of analytical grade.

Construction of plasmids and overexpression and purification of proteins. The *cmaA*, *cmaB*, *cmaC*, *cmaD* and *cmaE* genes were amplified from genomic DNA of *Pseudomonas syringae* pv. *tomato* DC3000 prepared with the Bactozol kit (Molecular Research Center, Inc.). The oligonucleotide pairs used for PCR amplification are described in Supplementary Table S1. His-tagged Cma proteins were overexpressed in *E. coli* BL21 (DE3) transformed with their respective overexpression plasmids.

His-tagged CmaA, CmaD and CmaE proteins were purified with Ni^{2+}-nitrilotriacetate (Ni^{2+}-NTA) agarose followed by gel filtration. For the CmaB and CmaC proteins, all cell-free preparations were manipulated under an inert atmosphere with an Mbraun Labmaster glovebox maintained at 2 p.p.m. O_2 or less. His-tagged CmaB and CmaC were purified by Ni^{2+}-NTA affinity chromatography. After proteolytic cleavage of the His tag, further purification was

performed by anion-exchange and gel-filtration chromatography performed with an Äkta Explorer 100 (GE Healthcare) configured to maintain an anaerobic atmosphere during purification, as described previously[28].

Metal analysis. The metal content of the CmaB and CmaC protein preparations was determined by inductively coupled plasma mass spectrometry (ICP-MS) performed by Phytronix Technologies. In reconstitution experiments, iron concentrations were determined colorimetrically with Ferene S (ref. 29).

Reconstitution of CmaB *in vitro*. Apo-CmaB was reconstituted anaerobically in the presence or absence of α-KG. CmaB was incubated with 1 mM dithiothreitol and 0.75 mM $Fe(NH_4)_2(SO_4)_2$ for 30 min. The protein was desalted on a Bio-Gel P6-DG column (Bio-Rad) equilibrated in 20 mM HEPES pH 7.5 to remove dithiothreitol and excess iron. When present, α-KG was added at 2 mM in both the initial incubation and the final storage buffer.

Aminoacylation assays for self-loading of CmaA and *in trans* loading of CmaD. Aminoacylation of CmaA and CmaD was monitored with two methods. In the first approach, the amino acid, ATP and proteins were mixed, a time course was performed and the reaction was quenched at different time points followed by liquid-scintillation counting of the resuspended pellets. In the second approach, SDS–PAGE gels of different reaction time points were performed, followed by autoradiography to measure the extent of protein labelling with L-[^{14}C]Val. The loading of holo-CmaD was investigated in the presence and absence of CmaE with CmaA. These assays were also performed with the CmaA(S542A) and CmaE(C105A) protein variants.

CmaB and CmaC activity assays. The reactions catalysed by CmaB and CmaC were investigated by incubating the enzymes with loaded CmaA with or without loaded CmaD. In incubations with loaded CmaA only, CmaA loaded with L-[^{3}H]*allo*-Ile was incubated with α-KG and CmaB with or without CmaC. Chloride was present in the reaction mixture. In incubations with loaded CmaD, the latter was prepared by incubating holo-CmaA with L-[^{3}H]*allo*-Ile or L-[^{14}C]Val, CmaE and ATP. α-KG and CmaB with or without CmaC were then added. Chloride was present in the reaction mixture. The resulting reactions were transferred to 0.5 ml Ultrafree centrifugal devices equipped with a 5-kDa membrane cut-off (Millipore). The extra amino acids were removed by using four wash steps with 0.5 ml of 20 mM HEPES pH 7.5. The resulting protein solution was incubated with the TycF type II thioesterase[11] (5 μM) to release the loaded amino acids. The amino acids were separated from the proteins by centrifuging the filter devices. The amino acids were then derivatized with *o*-phthalaldehyde and 3-mercaptopropionic acid (OPA reagent) as described previously in amino acid analysis[30] and analysed by radio-HPLC on a Beckman System Gold HPLC equipped with a Beckman 171 radioisotope detector and compared with authentic standards. The activities of CmaB and CmaC were also investigated on the free amino acids at a concentration of 100 μM with α-KG, O_2 and $MgCl_2$ present.

α-KG, Fe, O_2 and chloride dependence of the CmaB reaction. The α-KG, Fe, O_2 and chloride dependence of the CmaB reaction were investigated as described in Supplementary Methods.

Reaction product identification with LC–MS. The masses of the released L-*allo*-Ile, γ-Cl-L-*allo*-isoleucine and coronamic acid from CmaD using the TycF thioesterase were monitored after derivatization with the OPA reagent. Reactions (300 μl) of 100 μM CmaD were performed with CmaB with or without CmaC. The amino acids were hydrolysed as noted above and analysed by LC–MS (positive mode).

Received 22 March; accepted 12 May 2005.

1. Gribble, G. W. Natural organohalogens: a new frontier for medicinal agents? *J. Chem. Educ.* **81,** 1441–1449 (2004).
2. Buell, C. R. *et al.* The complete genome sequence of the *Arabidopsis* and tomato pathogen *Pseudomonas syringae* pv. *tomato* DC3000. *Proc. Natl Acad. Sci. USA* **100,** 10181–10186 (2003).
3. Parry, R. J., Lin, M. T., Walker, A. E. & Mhaskar, S. Biosynthesis of coronatine: investigations of the biosynthesis of coronamic acid. *J. Am. Chem. Soc.* **113,** 1849–1850 (1991).
4. Parry, R. J., Mhaskar, S. V., Lin, M. T., Walker, A. E. & Mafoti, R. Investigations of the biosynthesis of the phytotoxin coronatine. *Can. J. Chem.* **72,** 86–99 (1994).
5. Young, S. A., Park, S. K., Rodgers, C., Mitchell, R. E. & Bender, C. L. Physical and functional characterization of the gene cluster encoding the polyketide phytotoxin coronatine in *Pseudomonas syringae* pv. *glycinea*. *J. Bacteriol.* **174,** 1837–1843 (1992).
6. Couch, R., O'Connor, S. E., Seidle, H., Walsh, C. T. & Parry, R. Characterization of CmaA, an adenylation–thiolation didomain enzyme involved in the biosynthesis of coronatine. *J. Bacteriol.* **186,** 35–42 (2004).
7. Hegg, E. L. & Que, L. Jr The 2-His-1-carboxylate facial triad—an emerging structural motif in mononuclear non-heme iron(II) enzymes. *Eur. J. Biochem.* **250,** 625–629 (1997).
8. Koehntop, K. D., Emerson, J. P. & Que, L. Jr The 2-His-1-carboxylate facial triad: a versatile platform for dioxygen activation by mononuclear non-heme iron(II) enzymes. *J. Biol. Inorg. Chem.* **10,** 87–93 (2005).
9. Guenzi, E., Galli, G., Grgurina, I., Gross, D. C. & Grandi, G. Characterization of the syringomycin synthetase gene cluster. A link between prokaryotic and eukaryotic peptide synthetases. *J. Biol. Chem.* **273,** 32857–32863 (1998).
10. Chang, Z. *et al.* The barbamide biosynthetic gene cluster: a novel marine cyanobacterial system of mixed polyketide synthase (PKS)-non-ribosomal peptide synthetase (NRPS) origin involving an unusual trichloroleucyl starter unit. *Gene* **296,** 235–247 (2002).
11. Yeh, E., Kohli, R. M., Bruner, S. D. & Walsh, C. T. Type II thioesterase restores activity of a NRPS module stalled with an aminoacyl-*S*-enzyme that cannot be elongated. *Chembiochem* **5,** 1290–1293 (2004).
12. Schofield, C. J. & Zhang, Z. Structural and mechanistic studies on 2-oxoglutarate-dependent oxygenases and related enzymes. *Curr. Opin. Struct. Biol.* **9,** 722–731 (1999).
13. Hausinger, R. P. Fe^{II}/α-ketoglutarate-dependent hydroxylases and related enzymes. *Crit. Rev. Biochem. Mol. Biol.* **39,** 21–68 (2004).
14. Price, J. C., Barr, E. W., Tirupati, B., Bollinger, J. M. Jr & Krebs, C. The first direct characterization of a high-valent iron intermediate in the reaction of an α-ketoglutarate-dependent dioxygenase: a high-spin Fe(IV) complex in taurine/α-ketoglutarate dioxygenase (TauD) from *Escherichia coli*. *Biochemistry* **42,** 7497–7508 (2003).
15. Rohde, J. U. *et al.* Crystallographic and spectroscopic characterization of a nonheme Fe(IV) = O complex. *Science* **299,** 1037–1039 (2003).
16. Cook, G. K. & Mayer, J. M. C-H bond activation by metal oxo species: oxidation of cyclohexane by chromyl chloride. *J. Am. Chem. Soc.* **116,** 1855–1868 (1994).
17. Mayer, J. M. Hydrogen atom abstraction by metal-oxo complexes: understanding the analogy with organic radical reactions. *Acc. Chem. Res.* **31,** 441–450 (1998).
18. Kojima, T., Leising, R. A., Yan, S. & Que, L. Jr Alkane functionalization at nonheme iron center. Stoichiometric transfer of metal-bound ligands to alkane. *J. Am. Chem. Soc.* **115,** 11328–11335 (1993).
19. McCarthy, A. A., Baker, H. M., Shewry, S. C., Patchett, M. L. & Baker, E. N. Crystal structure of methylmalonyl-coenzyme A epimerase from *P. shermanii*: a novel enzymatic function on an ancient metal binding scaffold. *Structure* **9,** 637–646 (2001).
20. Armstrong, R. N. Mechanistic diversity in a metalloenzyme superfamily. *Biochemistry* **39,** 13625–13632 (2000).
21. Gerlt, J. A. & Babbitt, P. C. Divergent evolution of enzymatic function: mechanistically diverse superfamilies and functionally distinct suprafamilies. *Annu. Rev. Biochem.* **70,** 209–246 (2001).
22. Vaillancourt, F. H., Yin, J. & Walsh, C. T. SyrB2 in syringomycin E biosynthesis is a nonheme Fe^{II} α-ketoglutarate- and O_2-dependent halogenase. *Proc. Natl Acad. Sci. USA* **102,** 10111–10116 (2005).
23. Massey, V. Activation of molecular oxygen by flavins and flavoproteins. *J. Biol. Chem.* **269,** 22459–22462 (1994).
24. Bugg, T. D. Oxygenases: mechanisms and structural motifs for O_2 activation. *Curr. Opin. Chem. Biol.* **5,** 550–555 (2001).
25. Ryle, M. J. & Hausinger, R. P. Non-heme iron oxygenases. *Curr. Opin. Chem. Biol.* **6,** 193–201 (2002).
26. Entsch, B., Ballou, D. P. & Massey, V. Flavin–oxygen derivatives involved in hydroxylation by ρ-hydroxybenzoate hydroxylase. *J. Biol. Chem.* **251,** 2550–2563 (1976).
27. Yeh, E., Garneau, S. & Walsh, C. T. Robust *in vitro* activity of RebF and RebH, a two-component reductase/halogenase, generating 7-chlorotryptophan during rebeccamycin biosynthesis. *Proc. Natl Acad. Sci. USA* **102,** 3960–3965 (2005).
28. Vaillancourt, F. H., Han, S., Fortin, P. D., Bolin, J. T. & Eltis, L. D. Molecular basis for the stabilization and inhibition of 2, 3-dihydroxybiphenyl 1,2-dioxygenase by *t*-butanol. *J. Biol. Chem.* **273,** 34887–34895 (1998).
29. Haigler, B. E. & Gibson, D. T. Purification and properties of NADH-ferredoxin$_{NAP}$ reductase, a component of naphthalene dioxygenase from *Pseudomonas* sp. strain NCIB 9816. *J. Bacteriol.* **172,** 457–464 (1990).
30. Molnar-Perl, I. Derivatization and chromatographic behaviour of the *o*-phthaldialdehyde amino acid derivatives obtained with various SH-group-containing additives. *J. Chromatogr. A* **913,** 283–302 (2001).

Supplementary Information is linked to the online version of the paper at www.nature.com/nature.

Acknowledgements We thank M. R. Rondon for providing *Pseudomonas syringae* pv. *tomato* DC3000, and M. G. Thomas for discussion. This work was supported in part by an NIH grant (C.T.W.), a Merck-sponsored Fellowship of the Helen Hay Whitney Foundation (F.H.V.), an NSERC Postdoctoral Fellowship (F.H.V.), an NIH Medical Scientist Training Program Fellowship (E.Y.), a Jane Coffin Childs Memorial Fund for Medical Research Fellowship (D.A.V.), and an Irving S. Sigal Postdoctoral Fellowship (S.E.O.).

Author Information Reprints and permissions information is available at npg.nature.com/reprintsandpermissions. The authors declare no competing financial interests. Correspondence and requests for materials should be addressed to C.T.W. (christopher_walsh@hms.harvard.edu).